Pergamon

Int. J. Heat Mass Transfer. Vol. 40, No. 16, pp. 3981–3990, 1997

Printed in Great Britain
0017–9310/97 $17.00+0.00

PII: S0017–9310(97)00047–1

Numerical analysis of heat transfer and fluid flow in a three-dimensional wavy-fin and tube heat exchanger

JIIN-YUH JANG and LI-KWEN CHEN

Department of Mechanical Engineering, National Cheng-Kung University, Tainan, Taiwan 701, Republic of China

(*Received* 20 *July* 1996)

Abstract—The effects of different geometrical parameters, including tube row numbers (1–4 rows), wavy angles ($\theta = 8.95°$, 17.05°, 32.21°) and wavy heights ($S = 0.751$, 1.500 and 3.003 mm) are investigated in detail for the Reynolds number Re_H (based on the fin spacing and the frontal velocity) ranging from 400 to 1200. Numerical results indicate that the row effect is less important in a wavy-fin as compared to plain-fin counterpart. It is also found that, for equal wavy height, both the average Nusselt number and pressure coefficient are increased as the wavy angle is increased; while for equal wavy angle, they are decreased as the wavy height is increased. The combination of ($\theta = 8.95°$, $S = 1.500$ mm) gives the highest flow area goodness factor (j/f). A comparison of the numerical results with the available experimental data is also presented. © 1997 Elsevier Science Ltd.

1. INTRODUCTION

The plate-fin and tube heat exchangers are employed in a wide variety of engineering applications, for instance, in air conditioning units, process gas heaters and coolers, compressor intercoolers and aftercoolers, etc. Generally, a liquid flows through the tubes and a gas flows through the channels formed by the neighboring fins around the tube bank. The heat transfer between the gas and the fins and tube surfaces is determined by the flow structure which is three-dimensional. Wavy-fins are one of the very popular fin patterns that are developed to improve heat transfer performance. The wavy surface can lengthen the flow path of the air flow and cause better airflow mixing. Therefore, higher heat transfer performance is expected compared to plain plate fin surface.

There have been a number of numerical studies on the thermal–hydraulic characteristics for a two-dimensional wavy of corrugated channel flow. Nishimura *et al.* [1] used a finite element method to study a two-dimensional pulsatile flow in a wavy channel with periodically converging–diverging cross-sections. Xin and Tao [2] numerically analyzed the laminar fluid flow and heat transfer in two-dimensional wavy channels of uniform cross-sectional area. The laminar and turbulent boundary layer flows over a wavy wall have been numerically investigated by Patal *et al.* [3–4]. Rutledge and Sleicher [5] numerically studied the possibility of improving heat transfer rates by incorporating small corrugations into a two-dimensional channel.

Experimental studies of heat transfer and pressure drop in two-dimensional corrugated or wavy channels have been performed by several researchers. Goldstein and Sparrow [6] used the naphthalene sublimation technique to determine the local and average heat transfer characteristics for flow in a two-dimensional corrugated wall channel. The effect of rounding of protruding edges of a two-dimensional corrugated-wall duct was investigated by Sparrow and Hossfeld [7]. It was found that given a Reynolds number, the rounding of the corrugation peaks brought about a decrease in the Nusselt number and the friction factor decreased even more than did the Nusselt number. Ali and Ramadhyani [8] experimentally studied the convective heat transfer in the entrance region of two-dimensional corrugated channels. The Nusselt number in the corrugated channels exceeded those in the parallel-plate channels by approximately 140 and 240%, the corresponding increases in friction factor being 130 and 280%. Snyder *et al.* [9] investigated forced-convection heat transfer rates and pressure drops in the thermally fully developed region of a two-dimensional serpentine channel. On an equal Reynolds number basis, the heated surface of the serpentine channel outperformed the baseline parallel-plate channel by about a factor of 9 in air and 14 in water.

The reported thermal–hydraulic performance data of the wavy-fin and tube heat exchangers were experimental in nature. Yoshii [10] presented dry-surface Nusselt number data for two eight-row coil (one with in-line and one with staggered layout) with a wavy pattern. Later, Yoshii *et al.* [11] reported wet and dry surface data for two wavy-finned cooling coils. One coil had a two-row in-lined tube arrangement and the other had a two-row staggered tube arrangement.

NOMENCLATURE

C_P	pressure coefficient
$\overline{C_P}$	average pressure coefficient
f	friction factor $((p-p_{in})/\frac{1}{2}\rho w_{in}^2) \times (H/4L)$
h	heat transfer coefficient (W m^{-2} K^{-1})
H	fin spacing (mm)
L	flow length (mm)
j	Colburn factor $Nu/(Re_H Pr^{1/3})$
k	thermal conductivity (W m^{-1} K^{-1})
n	dimensionless unit normal vector
Nu	local Nusselt number, $(h \cdot H)/k$
$\overline{Nu}$	average Nusselt number
p	pressure in the xy-plane (Pa)
P	dimensionless pressure $(p-p_\infty)/\rho w_{in}^2$
Pr	Prandtl number, v/α
q''	heat flux (W m^{-2})
Re_H	Reynolds number, $(w_{in} \cdot H)/v$
S	wavy height (mm)
T	temperature (°C)
T_{in}	inlet temperature (°C)
T_w	wall temperature (°C)
T_b	bulk mean temperature (°C)
U	dimensionless velocity vectors
w_{in}	frontal velocity (m s^{-1}).

Greek symbols

α	thermal diffusivity, (m^2 s^{-1})
ρ	density of fluid (kg m^{-3})
v	kinematic viscosity (m^2 s^{-1})
θ	wavy angle
β	circumferential angle
Θ	dimensionless temperature $(T-T_w)/(T_{in}-T_w)$
Θ_b	dimensionless bulk mean temperature $(T_b-T_w)/(T_{in}-T_w)$.

They showed that a 20–40% increase in the heat transfer coefficient and a 50–100% increase in the pressure drop, for a wavy-finned cooling coil operating under wet-surface conditions. Beecher and Fangan [12] experimentally tested 27 fin-and-tube heat exchangers with 21 of them having wavy-fin geometry. Webb [13] used a multiple regression technique to correlate Beecher and Fangan [12] data. The Webb [13] correlation can predict 88% of the wavy-fin data within ±5% and 96% of the data within ±10%. An experimental study was conducted by Mirth and Ramadhyani [14] to determine the Nusselt number and friction factor on the air-side of wavy-finned, chilled-water cooling coil. General correlations of the dry and wet surfaces were presented. Recently, Wang *et al.* [15] made extensive experiments on the heat transfer and pressure drop characteristics of wavy-fin and tube heat exchangers.

The foregoing literature review shows that no related numerical work on the three-dimensional wavy-fin and tube heat exchangers has been published up to now. This has motivated the present investigation. The present study provides the numerical solutions for the actual multi-row (1 ~ 4 rows) wavy-fin and tube heat exchangers. Therefore, a whole computational domain from the fluid inlet to outlet is solved directly. The effects of different geometrical parameters, including tube row numbers, wavy angles and wavy heights are investigated in detail for the Reynolds number ranging from 400 to 1200. It should be noted that the corresponding problem for a plain-fin was recently solved by Jang *et al.* [16]. The present numerical results for the wavy-fin are compared with those of a plain-fin counterpart [16] and those obtained from the experiment by Wang *et al.* [15] conducted in a steady-state open wind tunnel.

2. MATHEMATICAL ANALYSIS

2.1. *Governing equations*

The dashed lines in Fig. 1(a) designate the computational domain. Assuming symmetry conditions on the mid-plane between two fins, the bottom and top boundaries simulate the fin and the mid-plane, respectively. The coordinate system is also illustrated in the Figure. Figure 1(b) shows the five different combinations of wavy angle ($\theta = 8.95$, 17.05, and 32.21°) and wavy heights ($S = 0.751$, 1.500 and 3.003 mm) used in the present study. The fluid is considered incompressible with constant physical properties and the flow is assumed to be laminar, steady, three-dimensional and no viscous dissipation. The dimensionless equations for continuity, momentum and energy may be expressed in tensor form as

$$\frac{\partial U_i}{\partial X_i} = 0 \tag{1}$$

$$\frac{\partial}{\partial X_j}(U_i U_j) = -\frac{\partial P}{\partial X_i} + \frac{1}{Re_H}[\nabla^2 U_i] \tag{2}$$

$$\frac{\partial}{\partial X_j}(\Theta U_j) = \frac{1}{Re_H Pr}[\nabla^2 \Theta]. \tag{3}$$

In the above equations, the velocity has been non-dimensionalized with the uniform inlet velocity w_{in} at the channel inlet, all length coordinates with the channel height (fin spacing) H, and the pressure with ρw_{in}^2. The dimensionless temperature is defined as $\Theta = (T-T_w)/(T_{in}-T_w)$. The Reynolds number is $Re_H = w_{in} \cdot H/v$ and Pr is the fluid Prandtl number, which is set to be equal to 0.736 in the present study.

2.2. *Boundary conditions*

Because the governing equations are elliptic in spatial coordinates, the boundary conditions are required

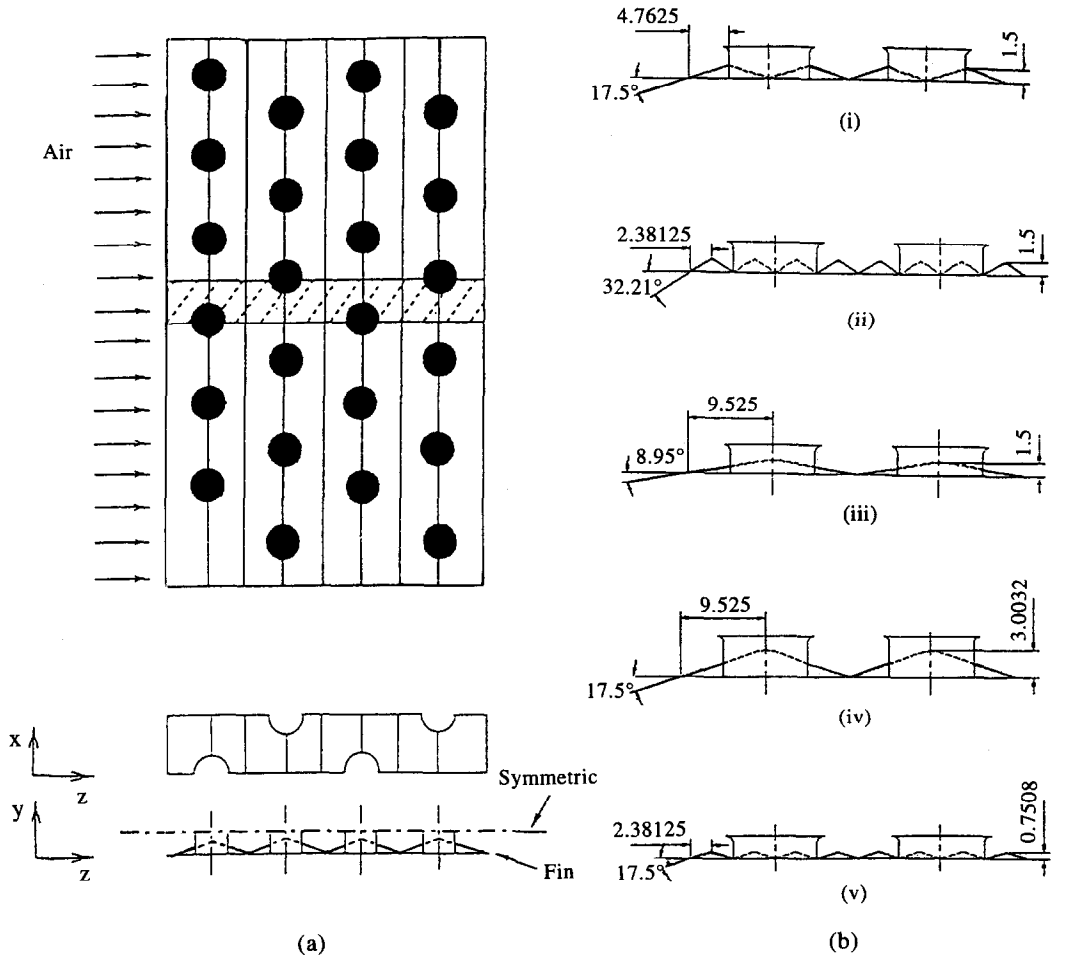

Fig. 1. (a) The computation domain and coordinate system; (b) five different combinations of wavy angle and wavy height.

for all boundaries of the computation domain. At the upstream boundary, uniform flow with velocity w_{in} and temperature T_{in} are assumed. At the downstream end of the computational domain, located seven times the tube diameter from the last downstream row cylinder, streamwise gradient (Neumann boundary conditions) for all the variables are set to zero. At the symmetry planes normal gradients are set to zero. At the solid surfaces, no-slip conditions and constant wall temperature T_w are specified.

The local pressure drop can be expressed in terms of the dimensionless pressure coefficient, C_p is defined as

$$C_p = \frac{p - p_{in}}{\frac{1}{2}\rho w_{in}^2} \tag{4}$$

where p_{in} is the pressure at inlet and L is the flow length.

The local heat transfer coefficient h is defined as

$$h = \frac{q''}{T_w - T_b} \tag{5}$$

where q'' is the local heat flux and T_b is the local bulk mean temperature of the fluid. The local heat transfer coefficient can be expressed in the dimensionless form by the Nusselt number Nu, defined as

$$Nu = \frac{h \cdot H}{k} = \left.\frac{\partial\left(\frac{\Theta}{\Theta_b}\right)}{\partial n}\right|_{wall} \tag{6}$$

where $\Theta_b = (T_b - T_w)/(T_{in} - T_w)$ is the local dimensionless bulk mean temperature and n is the dimensionless unit vector normal to the wall. The average pressure coefficient $\overline{C_p}$ Nusselt number $\overline{Nu}$ can be obtained by

$$\overline{C_p} = \frac{\int C_p \, dA_s}{\int dA_s} \tag{7}$$

$$\overline{Nu} = \frac{\int Nu \, dA_s}{\int dA_s} \tag{8}$$

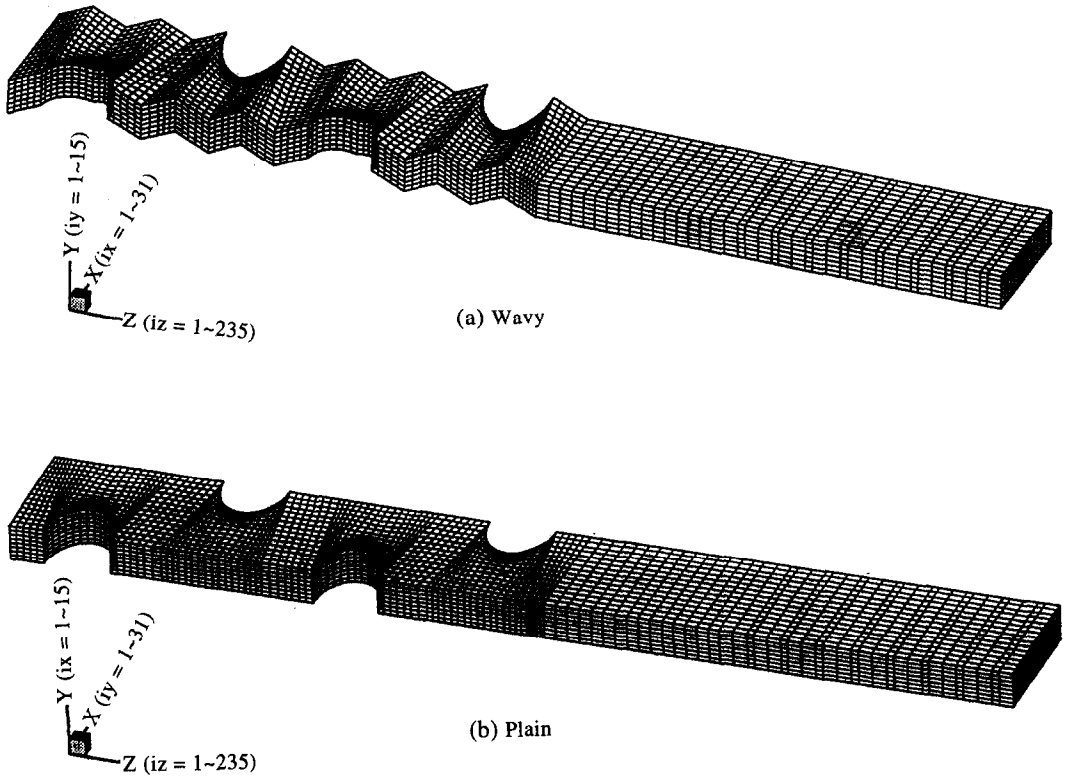

Fig. 2. Computation grid system.

where dA_s is the infinitesimal area of the wall surface. The friction factor f and Colburn factor j are defined as

$$f = \frac{p - p_{in}}{\frac{1}{2}\rho w_{in}^2} \times \frac{H}{4L} \tag{9}$$

$$j = \frac{\overline{Nu}}{Re_H Pr^{1/3}}. \tag{10}$$

3. NUMERICAL METHOD

In this study, the body-fitted coordinate system was used to generate a general curvilinear coordinate system numerically by solving Laplace equations with proper control of grid densities. The governing equations are solved numerically using a control volume based finite difference formulation. The SIMPLER algorithm [17] is used to solve iteratively the system of finite-difference equations. The hybrid scheme is employed for the treatment of convection and diffusion terms. A grid system of $31 \times 15 \times 235$ grid points is adopted typically in the computation domain for a four tube row arrangement as shown in Fig. 2. However, a careful check for the grid-independence of the numerical solutions has been made to ensure the accuracy and validity of the numerical results. For this purpose, three grid systems, $26 \times 11 \times 206$, $31 \times 15 \times 235$ and $33 \times 17 \times 259$, are tested. It is found that for $Re_H = 400$, the relative errors in the local and averaged Nusselt numbers between the solutions of $31 \times 15 \times 235$ and $33 \times 17 \times 259$ are less than 2%. Computations were performed on IBM RISC/6000 and typical CPU times are 6–7 h for each case.

4. RESULTS AND DISCUSSION

The numerical results for the actual wavy fin-and-tube heat exchangers with inlet frontal velocity 2.8 m s^{-1} ($Re_H = 600$) for the geometry having four-row deep, tube diameter 9.525 mm (3/8″), tube center spacing 29.4 mm, fin pitch 8 fins $in.^{-1}$ and with wavy angle $\theta = 17.05°$ and wavy heights $S = 1.500$ mm are shown in Figs 3–5. The corresponding numerical results for a plain-fin counterpart by Jang *et al.* [16] are also presented for the comparison. Figures 3 and 4 illustrate the streamline and the isotherm patterns for the wavy-fin and plain-fin arrangements on the xz-plane at $Y = 0.114$ (near the fin surface) and $Y = 1.591$ (near mid-plane between two fins), respectively. For the wavy-fin array, since the flow is repeatedly interrupted near the wavy surface, the flow structures near the fin surface (Fig. 3) are significantly different from that for a plain fin surface. It is also seen that the flow pattern and temperature contour on the xz-plane at $Y = 0.114$ (near the fin surface) and $Y = 1.591$ (near the mid-plane between two fins) are quite different. Near the fin surface, there is a smaller backflow zone at the rear of the tube; while near the mid-plane (Fig. 4), there is a larger recirculation zone behind the tube and the flow structures look similar to those for a

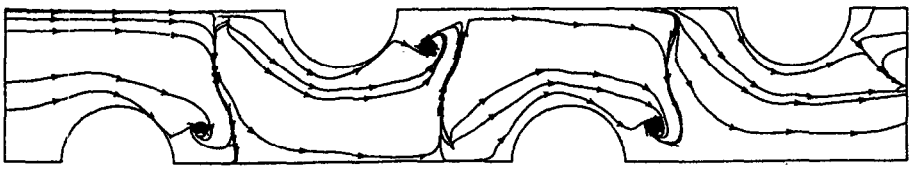

Streamline

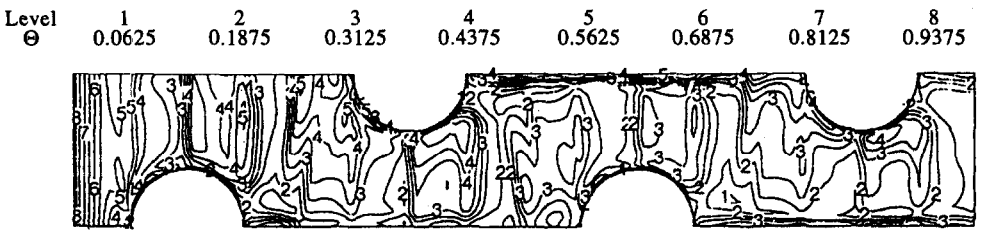

Isotherm

(a) Wavy

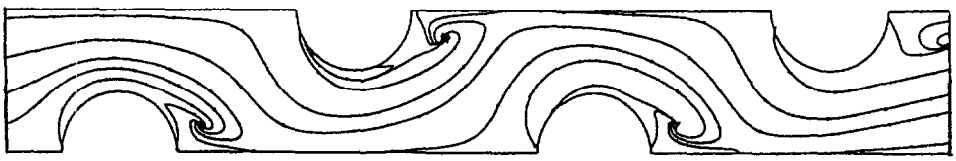

Streamline

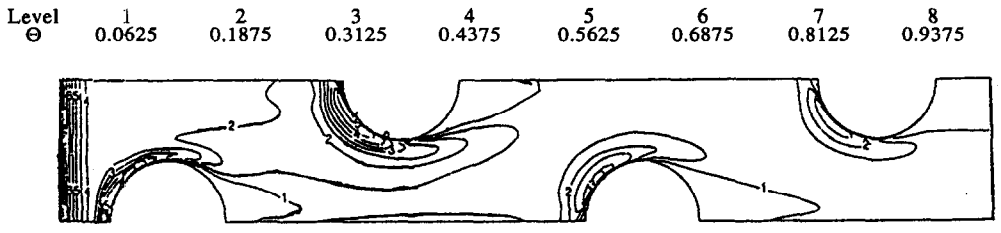

Isotherm

(b) Plain

Fig. 3. The streamline and isotherm patterns for the wavy and plain fin arrangements on the xz-plane at $Y = 0.114$ (near the fin surface) for $Re_H = 600$, $\theta = 17.05°$ and $S = 1.500$ mm.

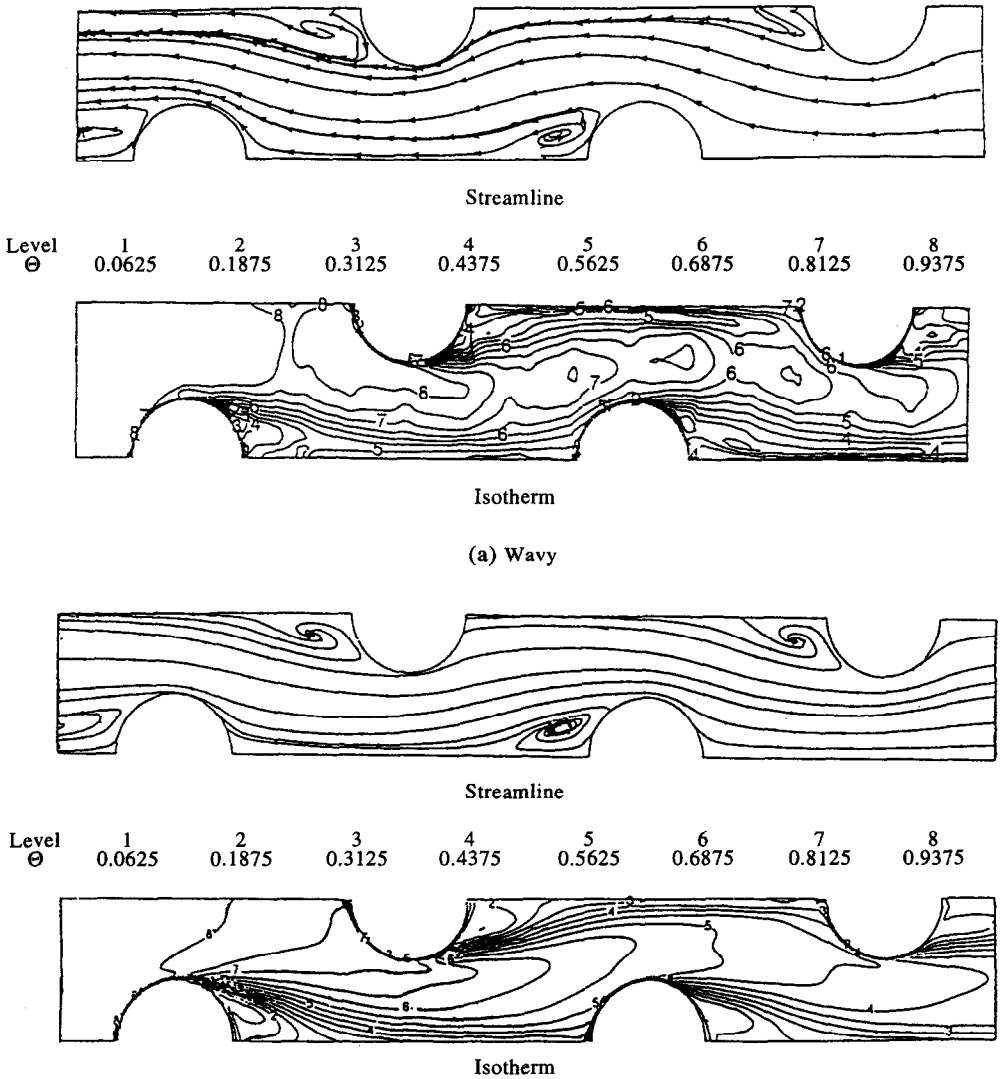

Fig. 4. The streamline and isotherm patterns for the wavy and plain fin arrangements on the xz-plane at $Y = 1.591$ (near the mid-plane between two fins) for $Re_H = 600$, $\theta = 17.05°$ and $S = 1.500$ mm.

plain-fin surface. Figure 5 presents the variations of C_p and Nu around the tube surface from the first to the fourth tube at $Y = 0.8525$ for both the wavy- and plain-fin arrays. The angle β is measured from front stagnation point of the tube. One can see that variations of the surface pressure profile for each tube look similar and the C_p value decreases in order from the first tube to the fourth tube. As expectedly, the wavy-fin tube array has a larger Nusselt number than plain-fin array. It is interesting to note that for a wavy-fin, the second tube has a maximum Nusselt number due to the interrupt of the boundary layer behind the first tube, while for a plain-fin, the Nu decreases in order from the first tube to the fourth tube.

In order to verify the validities of the present 3-D laminar model and numerical predictions, the calculated Colburn factor j and friction factor f vs Re_H as illustrated in Fig. 6 are compared with the available experimental data [15] for the geometry having four-row deep, tube diameter 9.525 mm, tube center spacing 29.4 mm, fin pitch 8, 11, 15 fins in.$^{-1}$ and with wavy angle $\theta = 17.05°$ and wavy heights $S = 1.500$ mm. The dashed lines denote the results for the corresponding plain-fin array counterpart. It is seen that the numerical results agree well with the experimental data [15]. The numerical results demonstrate that the Colburn factor j of wavy-fin arrangement is higher 63–71% than that of plain-fin arrangement, while the friction factor f of wavy-fin configuration is higher 75–102% than that of plain-fin configuration.

The tube row $N(N = 1–4$ rows) effects on the Colburn factor j and friction factor f as a function of Re_H

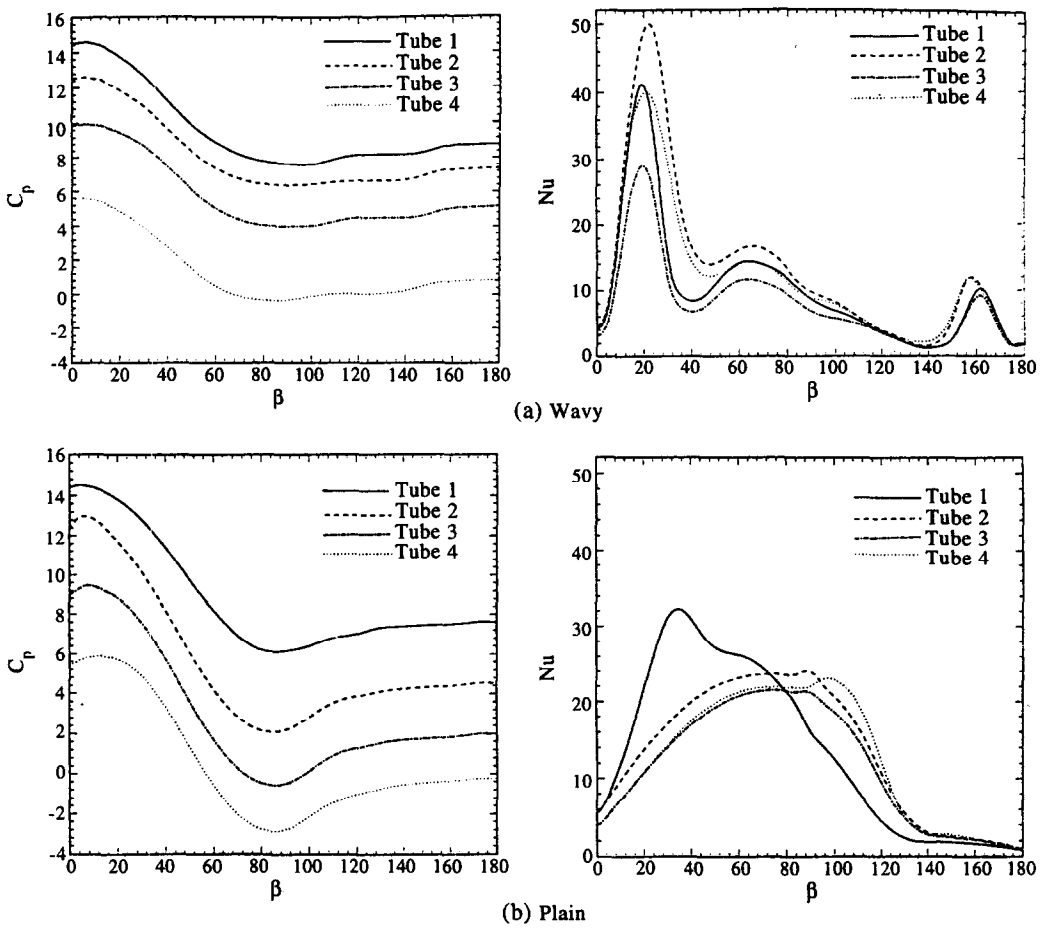

Fig. 5. The variations of C_p and Nu around tube surface at $Y = 0.8525$ for wavy and plain arrangements, $Re_H = 600$, $\theta = 17.05°$ and $S = 1.500$ mm.

are illustrated in Figs. 7(a, b), respectively, for tube diameter 9.525 mm, tube center spacing 29.4 mm, fin pitch 8 fins in.$^{-1}$ and with wavy angle $\theta = 17.05°$ and wavy height $S = 1.500$ mm. The experimental results by Wang *et al.* [15] are also depicted in the figure for comparison. It is seen that both the j and f are decreased as the number of tube rows increase from 1 to 4. It is also found that the j is nearly independent of the tube row number as $N > 3$. It should be noted that for a plain-fin surface, the tube row effect is insignificant as $N > 4$ [16]. Therefore, the row effect is less important in a wavy-fin as compared to plain-fin counterpart. Moreover, it is observed that the row effect is diminished as the Reynolds number Re_H is increased, due to a better mixing of the flow. This trend is also experimentally confirmed by Wang *et al.* [15] as shown in the figure.

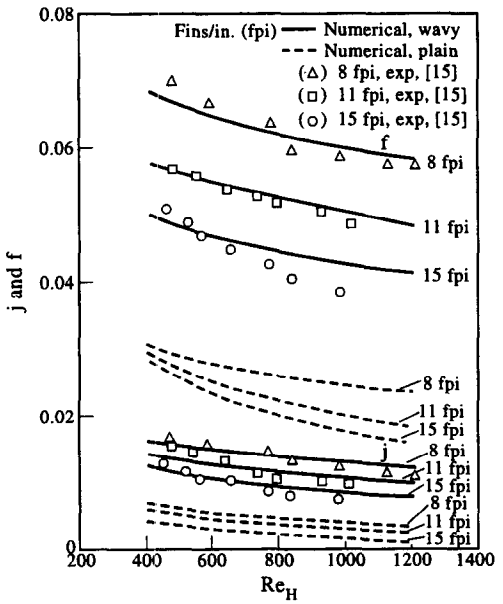

Fig. 6. The j and f vs Re_H for $\theta = 17.05°$ and $S = 1.500$ mm.

The effects of three different wavy angles ($\theta = 8.95$, 17.05 and 32.21°) on the average Nusselt number $\overline{Nu}$ and pressure coefficient $\overline{C_p}$ as a function of Re_H are shown in Fig. 8 (a, b), respectively, for the geometry having four-row deep, tube diameter 9.525 mm, tube center spacing 29.4 mm, fin pitch 8 fins in.$^{-1}$ and with fixed wavy heights $S = 1.500$ mm. Similarly, Fig. 9(a, b) show the effects of three different wavy heights ($S = 0.751$, 1.500 and 3.003 mm) on $\overline{Nu}$ and $\overline{C_p}$, respectively as a function of Re_H with fixed value of

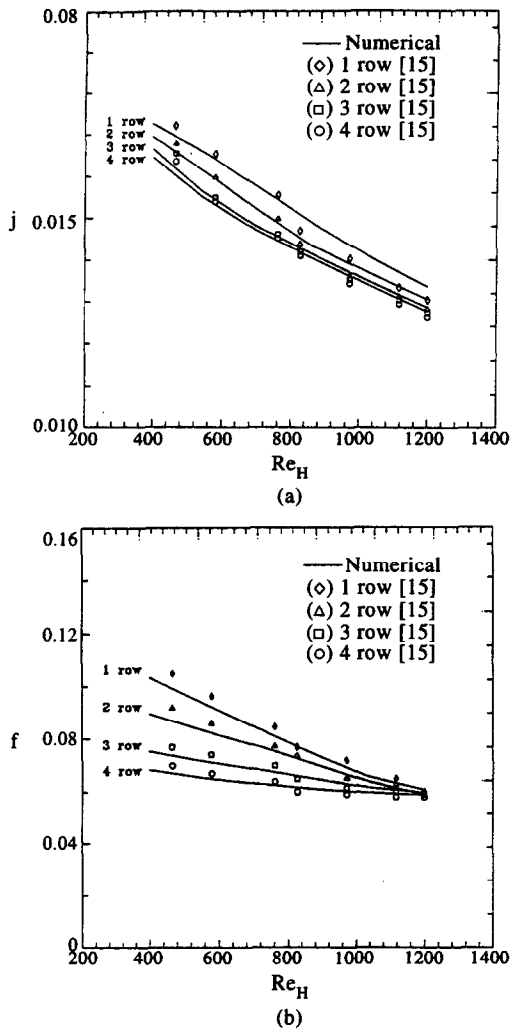

Fig. 7. The tube row effects on the j and f as a function of Re_H for $\theta = 17.05°$ and $S = 1.500$ mm.

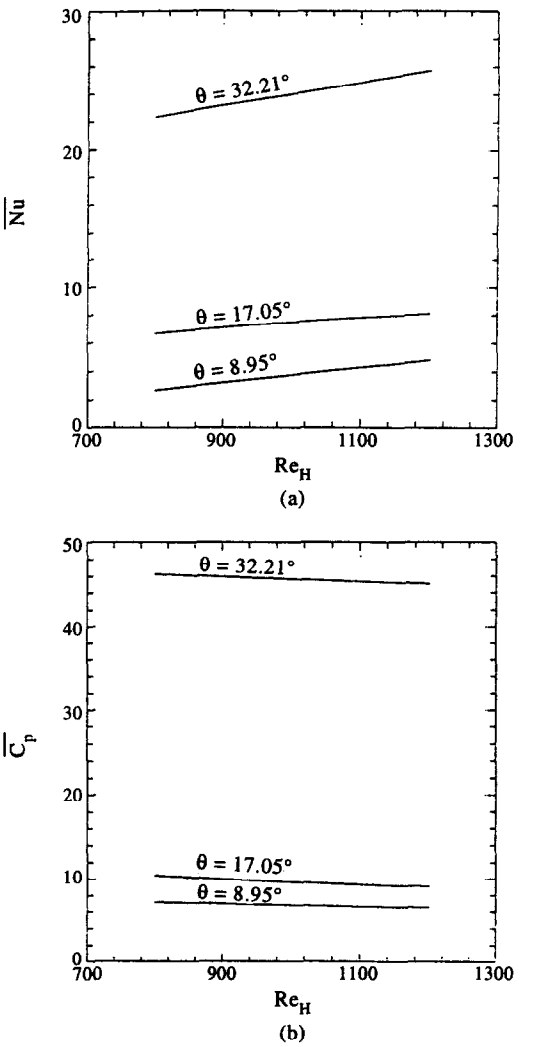

Fig. 8. The effects of three different wavy angles on the $\overline{Nu}$ and $\overline{C_p}$ as a function of Re_H for $S = 1.500$ mm.

wavy angle $\theta = 17.05°$. It is shown that, for equal wavy height, both the average Nusselt number and pressure coefficient are increased as the wavy angle is increased; while for equal wavy angle, they are decreased as the wavy height is increased. This is due to the fact that, for fixed wavy height or wavy angle, as the wavy angle increases or wavy height decreases, the wavelength of the wavy corrugations decreases, resulting in more wavy corrugation for a given flow length and, hence, the boundary layer is interrupted more frequently.

The flow area goodness factor is defined by London [18] as the ratio of the Colburn factor (j) to friction factor (f), j/f. A surface having a higher j/f factor is 'good', because it will require a lower free flow area and hence a lower frontal area for the exchanger. The variations of j/f with Re_H for the five different combinations of wavy angles ($\theta = 8.95$, 17.05 and 32.21°) and wavy heights ($S = 0.751$, 1.500 and 3.003 mm) used in the present study are presented in Fig. 10. It is seen that the flow goodness factor j/f varies from 0.05 for ($\theta = 32.21°$, $S = 1.500$ mm) to 0.20 for ($\theta = 8.95°$, $S = 1.500$ mm). One can observe that the more wavy corrugations for a given flow length, the lower value of the j/f factor. The commercial wavy-fin and tube heat exchanger ($\theta = 17.05°$, $S = 1.500$ mm) tested in Wang *et al.* [15] gives the third highest j/f value.

5. CONCLUSION

Fluid flow and heat transfer over a multi-row wavy fin-and-tube heat exchangers are studied numerically. Flow is laminar and three-dimensional and a whole computational domain from the fluid inlet and outlet is solved directly. The numerical results demonstrate that the Colburn factor of wavy-fin arrangement is higher 63–71% than that of plain-fin counterpart, while the friction factor of wavy-finned configuration is higher 75–102% than that of plain-finned configuration. For a four-row wavy-fin array, the second tube has a maximum Nusselt number, while for a

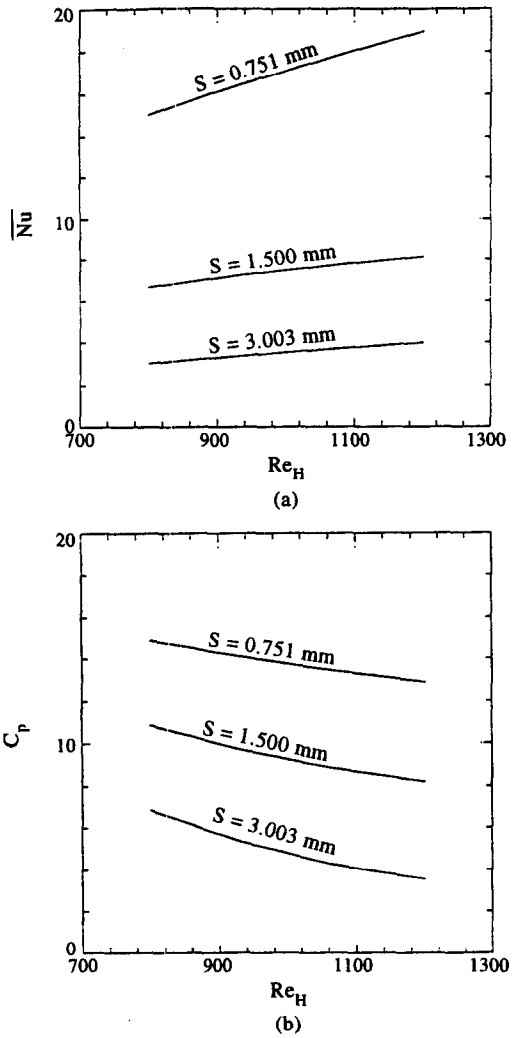

Fig. 9. The effects of three different wavy heights on the $\overline{Nu}$ and $\overline{C_p}$ as a function of Re_H for $\theta = 17.05°$.

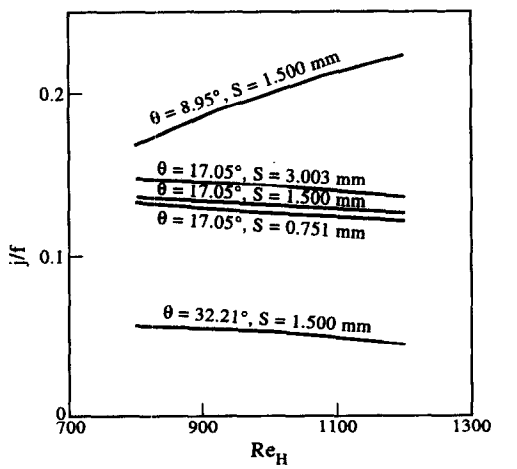

Fig. 10. The j/f vs Re_H for five different combinations of wavy angle and wavy height.

plain-fin, the *Nu* decreases in order from the first tube to the fourth tube. The row effect is less significant in a wavy-fin in comparison to a plain-fin and it will diminish with the increase of Reynolds number. For equal wavy height, both the average Nusselt number and pressure coefficient are increased as the wavy angle is increased; while for equal wavy angle, they are decreased as the wavy height is increased. It is also shown that the more wavy corrugations for a given flow length, the lower value of the flow area goodness factor. Good agreement between the numerical predictions and available experimental data is obtained.

Acknowledgements—Financial support for this work was provided by the National Science Council of Taiwan, under contract NSC 85-2212-E006-077.

REFERENCES

1. Nishimura, T., Yoshino, T. and Kawamura, Y., Numerical flow analysis of pulsatile flow in a channel with symmetric wavy walls at moderate Reynolds numbers. *Journal of Chemical Engineering of Japan*, 1987, **20**(5), 479–485.
2. Xin, R. C. and Tao, W. Q., Numerical prediction of laminar flow and heat transfer in wavy channels of uniform cross-section area. *Numerical Heat Transfer*, 1988, **14**, 465–481.
3. Patel, V. C., Chon, J. T. and Yoon, J. Y., Laminar flow over wavy walls. *Transactions of the ASME*, 1991, **113**, 574–578.
4. Patel, V. C., Chon, J. T. and Yoon, J. Y., Turbulent flow over wavy walls. *Journal of Fluids Engineering*, 1991, **113**, 574–586.
5. Rutledge, J. and Sleicher, C. A., Direct simulation of turbulent flow and heat transfer in a channel. Part II: a Green's function technique for wavy walls. *Communications in Numerical Methods in Engineering*, 1994, **10**, 489–496.
6. Goldstein, L. and Sparrow, J. M. E., Heat/mass transfer characteristics for flow in a corrugated wall channel. *Journal of Heat Transfer*, 1977, **99**, 187–195.
7. Sparrow, E. M. and Hossfeld, L. M., Effect of rounding of protruding edges on heat transfer and pressure drop in a duct. *International Journal of Heat and Mass Transfer*, 1984, **27**(10), 1715–1723.
8. Ali, M. M. and Ramadhyani, S., Experiments on convection heat transfer in corrugated channels. *Experimental Heat Transfer*, 1992, **5**, 175–193.
9. Snyder, B., Li, K. T. and Wirtz, R. A., Heat transfer enhancement in a serpentine channel. *International Journal of Heat and Mass Transfer*, 1993, **36**(12), 2965–2976.
10. Yoshii, T., Transient testing technique for heat exchangers fin surfaces. *Heat Transfer Japanese Research*, 1972, **1**(3), 51–58.
11. Yoshii, T., Yamamoto, M. and Otaki, T., Effects of dropwise condensate on wet surface heat surface heat transfer for air cooling oils. *Proceedings of the 13th International Congress of Refrigeration*, 1973, pp. 285–292.
12. Beecher, D. T. and Fagan, T. J., Effects of fin pattern on the air side heat transfer coefficient in plate finned-tube heat exchangers. *ASHRAE Transaction*, 1987, **93**(2), 1961–1984.
13. Webb, R. L., Air side heat transfer correlations for flat and wavy plate fin-and-tube geometries. *ASHREA Transaction*, 1990, **96**(2), 445–449.
14. Mirth, D. R. and Ramadhyani, S., Correlation for predicting the air-side Nusselt numbers and friction factor in

chilled water cooling coils. *Experimental Heat Transfer*, 1994, **7**, 143–162.
15. Wang, C. C., Fu, W. L. and Chang, C. T., Finned tube heat exchangers: wavy fin geometry. *Proceedings of the Asia Pacific Conference on Built Environment*, Vol. 1, Singapore, June 1–3 1995, pp. 194–204.
16. Jang, J. Y., Wu, M. C. and Chang, W. J., Numerical and experimental studies of three-dimensional plate-fin and tube heat exchangers. *International Journal of Heat and Mass Transfer*, 1996, **39**(10), 3057–3066.
17. Patakar, S. V., A calculation procedure for two-dimensional elliptic problems. *Numerical Heat Transfer*, 1981, **4**, 409–426.
18. London, A. L., Compact heat exchanger: part 2—surface geometry. *Mechanical Engineering*, 1964, **86**, 31–34.